Crystallisation of Glycine from Binary Solvent under Acoustic Levitation

Adriana Alieva[1], Matthew Boyes[1], Thomas Vetter[2], Cinzia Casiraghi[1*]

[1] School of Chemistry, University of Manchester, Manchester, UK
[2] School of Chemical Engineering and Analytical Science, University of Manchester, Manchester, UK

* Corresponding author: cinzia.casiraghi@manchester.ac.uk

Supplementary Information

S1. State-of-the-art for crystallisation from acoustic levitation

Reference	Compound Studied	In situ	Ex situ	Main results
[1]	Mannitol	CCD camera	Scanning electron microscopy (SEM)	Development of a mechanistic model to describe the drying behaviour and particle shell formation of drying droplets of multicomponent mixtures.
[2]	Sodium chloride	CCD camera		The salt solution droplets exhibit a two-stage evaporation process, involving water evaporation and salt precipitation. A higher concentration of salt and larger diameter of droplets led to a lower evaporation rate.
[3]	Mannitol, Trehalose, and Catalase	CCD camera	SEM	The morphology of the products from levitation experiments show a strong similarity to the crystals obtained from spray-drying indicating some suitability of the levitator as a model for spray-drying.
[4]	Sodium chloride, Ammonium chloride, Lysozyme, and Proteinase K	CCD cameras	Optical microscopy	Crystals obtained from the acoustically levitated droplets exhibits higher growth rates, larger sizes, better shapes, fewer crystals, as well as fewer twins and shards, compared with the control on a vessel wall.
[5]	Sodium chloride	Energy-dispersive X-ray diffraction (EDXD)		The transformation of sodium chloride to a polycrystalline state was observed.
[6]	Ascorbic acid, Acetylsalycic acid, Apoferritin, and Colloidal gold	Small- and wide angle X-ray scattering (SAXS/WAXS)		Did not provide much insight on the crystallisation process of ascorbic acid and acetylsalycic acid. The correct diffraction peaks of the resulting crystals from both molecules were observed.
[7]	Calcium carbonate ($CaCO_3$)	Wide angle X-ray scattering (WAXS)	Different stages characterized by transmission electron microscopy (TEM) and cryogenic-SEM	Detected the formation of amorphous liquid-like structures at early stage of the crystallization of $CaCO_3$. The primary particles form homogenously within the volume of the droplet and serving as a second step templates for the crystallization of calcite.

			and SEM	
[8]	Caffeine on substrates (glass, polystyrene, and polyester)		Atomic Force Microscopy (AFM) and SEM	• Both crystal modifications (α- and *β*-caffeine) are present
	Caffeine from levitation experiments	WAXS		• Only α –form was obtained Due to the continuous diffusion and mixture process in the acoustic field the continuous growth of germs is inhibited thus the crystallization starts at the entire volume of the levitated droplet simultaneously.
[9]	Nifedipine in different solvents	XRD and Raman spectroscopy	Raman spectroscopy	Detected intermediate forms depending on the solvent used. The metastable β-form is favoured when the formation of H bonds between solvent and solute is possible and the glassy form is built whenever formation of H bonds is not an option. Both intermediate phases lead to the formation of the α-form.
[10]	ROY(5-methyl-2-[(2-nitrophenyl)amino]-3-thiophenecarbonitrile) in different solvents	WAXS and Raman		Different intermediate forms and polymorphs of ROY were observed depending on the solvent used. Thus they suggest that the crystallization of a specific polymorph can be attributed to nearest neighbour interactions and intermolecular attractive forces between solvent and analyte.
[11]	Paracetamol (acetaminophen)	WAXS and Raman		Based on the choice of the solvent selective crystallisation of both forms of paracetamol (the monoclinic form I and the metastable form II) was achieved. Two different amorphous stages were identified: which transforms to different polymorphs at later stages.

S2. Acoustic Levitation Setup

Figure S2 shows a schematic representation of the acoustic levitation set-up used for our crystallisation studies. The system consists of an ultrasonic droplet levitator operating at 100 kHz (Tec5, Germany), a CCD camera (Allied Vision Manta G505B), backlight illumination and a controlled evaporator unit (Bronkhorst, CEM202A). The emitter and the reflector are encased in a chamber which is surrounded by a heating jacket to achieve environmental control. The heating jacket is connected to a water bath (Ministat 230, Huber, Germany) allowing the flow of temperature regulated water around the levitation chamber. Conditioned N_2 gas is introduced to the chamber at a controlled gas flow rate, temperature and humidity. The temperature and relative humidity within the levitation chamber were monitored with the use of an iButton temperature and humidity sensor (Thermochron). The flow rate of N_2 gas was set high enough to maintain the environmental control within the chamber without agitating the levitating droplet. The inner diameter of the chamber is 70 mm, with two sealable access windows of diameter of 25 mm, which allow imaging and droplet suspension in the acoustic field. A droplet was injected in the levitator using a Hamilton 1800 syringe. All levitation experiments were captured with a CCD camera.

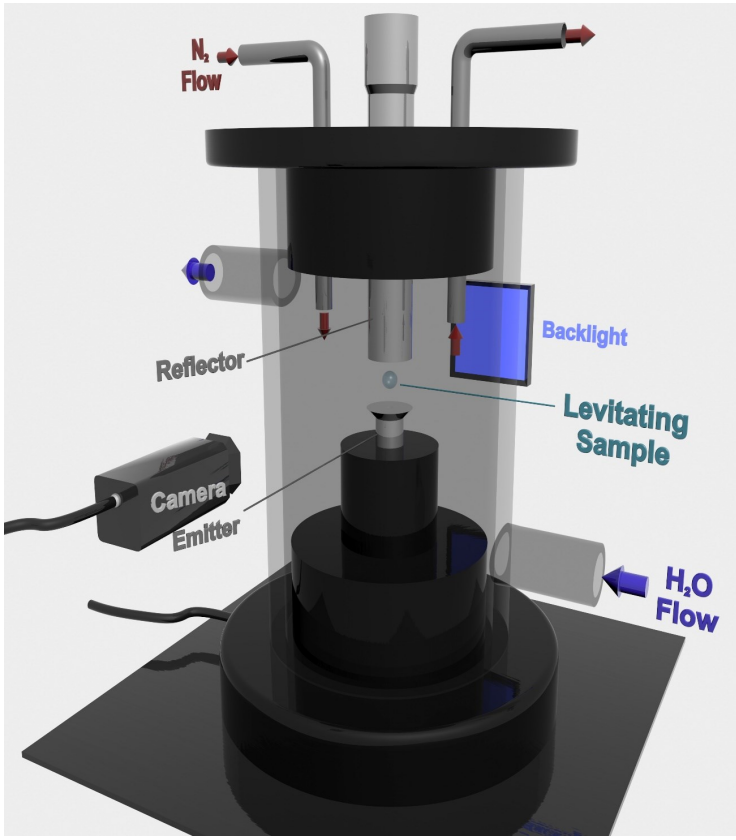

Figure S2. Schematic representation of the acoustic levitation setup.

S3. Evaporation profiles of glycine microdroplets from H_2O:IPA solvent system

Figure S3 shows the evaporation profiles of glycine microdroplets from H_2O:IPA solvent system. It can be clearly seen that both evaporation profiles of the binary solvent mixture for crystals obtained as spherical and non-spherical follow a similar trend.

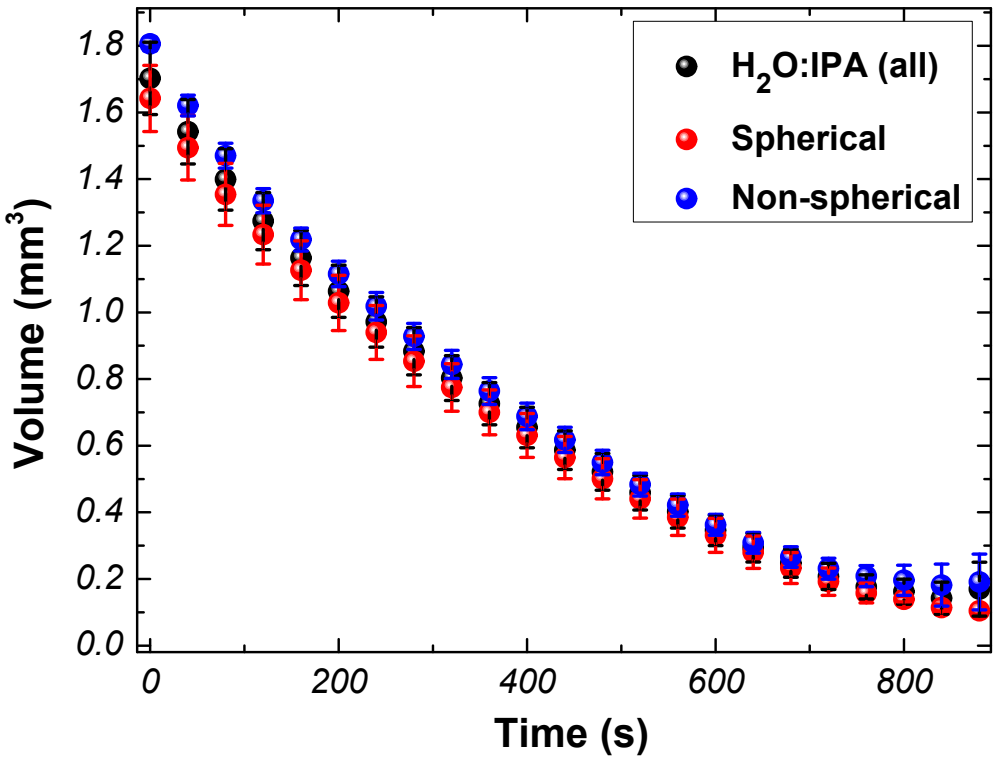

Figure S3. Evaporation profiles of glycine microdroplets from H_2O:IPA solvent system

S4. Characterisation protocol for polymorph screening

Figure S4 shows a schematic of the characterisation protocol developed for polymorph screening of glycine samples based on Raman spectroscopy. The procedure can be summarised as follows:

i) Mounting a glycine sphere on a substrate

ii) Taking Raman measurements from the outside of the sphere

iii) Cutting the sample into half using Laser Cutter

iv) Taking Raman measurements from the inner part of the sphere

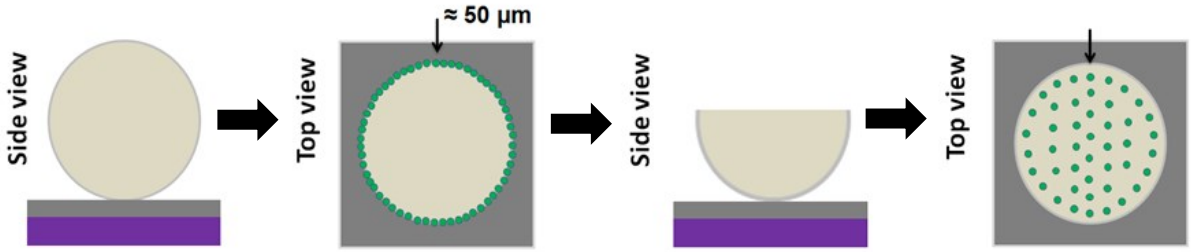

Figure S4. Schematic of the characterisation protocol for the polymorph screening of glycine samples.

S5. Raman spectrum of glycine polymorphs

Figure S5 shows the distinct Raman spectra of the CH region (2900-3050 cm^{-1}) of the three polymorphs of glycine. These peaks represent the symmetric (lower shift) and asymmetric (higher shift) stretches of the C-H bonds. The positions of these modes are distinct for each polymorph, which were found to be at 2972-3007 cm^{-1} for α-form, at 2953-3008 cm^{-1} for β-form and at 2962- 3000 cm^{-1} for γ-form.

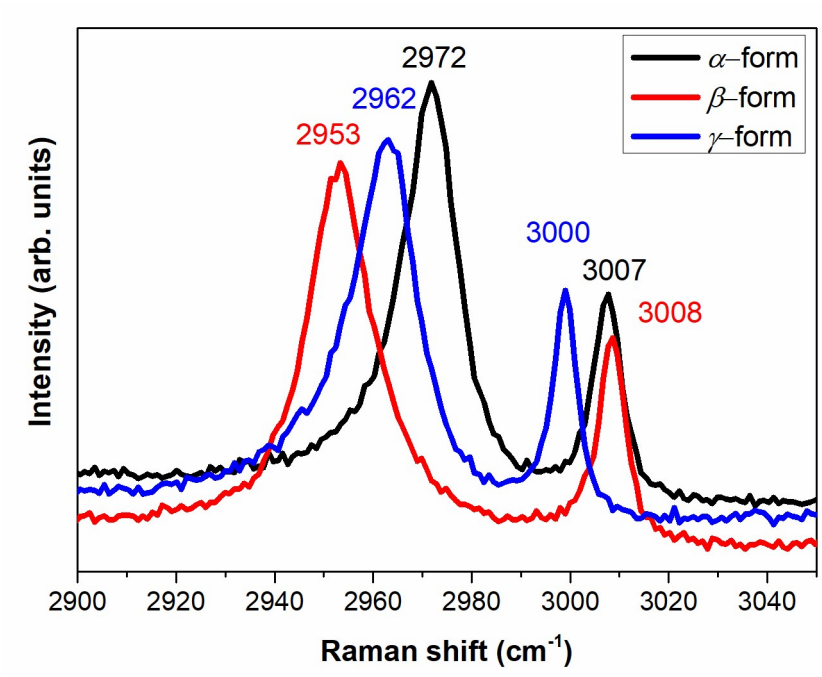

Figure S5. Raman spectra of glycine polymorphs.

S6. Fitting results of polymorphs obtained from different solvent systems

The fitting results for the position and Full Widths at Half Maximum (FWHM) of symmetric CH stretch (ν_s(CH)) and asymmetric CH stretch (ν_{as}(CH)) of Raman measurements taken from different regions of glycine crystals are shown in Table S1.

Table S1. Fitting results of the CH stretching modes of glycine crystals obtained from different solvent systems

Sample	**ν_s(CH)**		**ν_{as}(CH)**	
	Position (cm^{-1})	**FWHM (cm^{-1})**	**Position (cm^{-1})**	**FWHM (cm^{-1})**
H_2O out	2972	13	3008	5.7
H_2O centre	2971.68	12.8	3007	5.2
H_2O:IPA out	2971.60	12.8	3007	5.1
H_2O:IPA centre	2971.63	12.7	3007	5

References

[1] T. Abdullahi, Hassan; Burcham, Christopher; Vetter, "A mechanistic model to predict droplet drying history and particle shell formation in multicomponent systems," *Chem. Eng. Sci.*, vol. 224, 2020.

[2] Y. Maruyama and K. Hasegawa, "Evaporation and drying kinetics of water-NaCl droplets via acoustic levitation," *RSC Adv.*, vol. 10, no. 4, pp. 1870–1877, Jan. 2020, doi: 10.1039/c9ra09395h.

[3] H. Schiffter and G. Lee, "Single-droplet evaporation kinetics and particle formation in an acoustic levitator. Part 2: Drying kinetics and particle formation from microdroplets of aqueous mannitol, trehalose, or catalase," *J. Pharm. Sci.*, vol. 96, no. 9, pp. 2284–2295, 2007, doi: 10.1002/jps.20858.

[4] H.-L. Cao *et al.*, "Rapid crystallization from acoustically levitated droplets," *J. Acoust. Soc. Am.*, vol. 131, no. 4, pp. 3164–3172, 2012, doi: 10.1121/1.3688494.

[5] J. Leiterer, W. Leitenberger, F. Emmerling, A. F. Thünemann, and U. Panne, "The use of an acoustic levitator to follow crystallization in small droplets by energydispersive X-ray diffraction," *J. Appl. Crystallogr.*, vol. 39, no. 5, pp. 771–773, 2006, doi: 10.1107/S0021889806024915.

[6] J. Leiterer, F. Delißen, F. Emmerling, A. F. Thünemann, and U. Panne, "Structure analysis using acoustically levitated droplets," *Anal. Bioanal. Chem.*, vol. 391, no. 4, pp. 1221–1228, 2008, doi: 10.1007/s00216-008-2011-2.

[7] S. E. Wolf, J. Leiterer, M. Kappl, F. Emmerling, and W. Tremel, "Early homogenous amorphous precursor stages of calcium carbonate and subsequent crystal growth in levitated droplets," *J. Am. Chem. Soc.*, vol. 130, no. 37, pp. 12342–12347, 2008, doi: 10.1021/ja800984y.

[8] J. Leiterer, F. Emmerling, U. Panne, W. Christen, and K. Rademann, "Tracing coffee tabletop traces," *Langmuir*, vol. 24, no. 15, pp. 7970–7978, 2008, doi: 10.1021/la800768v.

[9] M. Klimakow *et al.*, "Combined synchrotron XRD/Raman measurements: In situ identification of polymorphic transitions during crystallization processes," *Langmuir*, vol. 26, no. 13, pp. 11233–11237, 2010, doi: 10.1021/la100540q.

[10] T. Gnutzmann, Y. Nguyen Thi, K. Rademann, and F. Emmerling, "Solvent-triggered crystallization of polymorphs studied in situ," *Cryst. Growth Des.*, vol. 14, no. 12, pp. 6445–6450, 2014, doi: 10.1021/cg501287v.

[11] Y. Nguyen Thi, K. Rademann, and F. Emmerling, "Direct evidence of polyamorphism in paracetamol," *CrystEngComm*, vol. 17, no. 47, pp. 9029–9036, 2015, doi: 10.1039/c5ce01583a.